MATTER: International Journal of Science and Technology
ISSN 2454-5880

Kashani and Zolfaghari, 2018

Volume 4 Issue 2, pp. 182-199

Date of Publication: 20th September 2018

DOI-https://dx.doi.org/10.20319/mijst.2018.42.182199

This paper can be cited as: Kashani, H. M., & Zolfaghari, A. (2018). A Comparison of Estimated Life of Knee Implant Applying the Multiaxial Fatigue Criteria. MATTER: International Journal of Science and Technology, 4(2), 182-199.

A COMPARISON OF ESTIMATED LIFE OF KNEE IMPLANT APPLYING THE MULTIAXIAL FATIGUE CRITERIA

H. Moayeri Kashani
Department of Mechanical Engineering, Tehran West Branch, Islamic Azad University, Tehran, Iran
Moayeri.Hamed@wtiau.ac.ir

A. Zolfaghari
Department of Mechanical Engineering, Tehran West Branch, Islamic Azad University, Tehran, Iran
A.Zolfaghari66@gmail.com

Abstract

The experience of losing a part of body is very painful and irritating, many factors, such as sports injuries, arthro-rheumatoid arthritis, weight gain, car accidents, and the like can sometimes lead to the destruction of joints and knee tissues. Today the most successful and fastest process to assist these people is the introduction of total knee replacement. Therefore, the evaluation of the materials used and the life estimation of knee implants used in total knee replacement are of particular importance. This article investigates the stress analysis and life estimation of knee implants in multiaxial loading. For this purpose, the tibia and femur were modeled using the results of the CT scan of a completely normal sample, and using the Solidworks software, followed by modelling implant sections and other sets. The analysis of stress and application of problem conditions were done in Abaqus finite element analysis software and life estimation was done using coding in MATLAB software. Based on the walking cycle, the minimum load of 200 N and maximum of 2600 N was applied to metatarsus in standing

position, and finally, using stress analysis and multiaxial fatigue criteria such as Von Mises, the maximum principal stresses, maximum shear stress (Tresca), maximum principal strain, Brown Miller, Fatemi-Socie and Smith Watson Topper, the life of the implant was estimated and the results were compared. Ultimately, the longest life expectancy was estimated on the basis of the Tresca criterion and the shortest life span on the basis of the Smith Watson-Topper criteria.

Keywords

Critical Plane Fatigue Criteria, Fatigue, Finite Element Analysis, Knee Implant, Multiaxial Fatigue Criteria

1. Introduction

During total knee replacement, the knee implant replaces the defective joints and parts of the knee, and it will be placed between the femur and tibia. Relative integrity of implant components with femur and tibia takes about 6 week. In the early 1970s, the concept of replacing tibiofemoral condylar surfaces with cemented fixation was developed and refined, along with preservation of the cruciate ligaments, and for correcting severe knee deformation, condylar knee was introduced with posterior cruciate ligament and in the early 1974, replacing patellofemoral joint had become standard practice either by preserving or sacrificing the cruciate ligaments (Ranawat & Ranawat, 2012). Locating and choosing the right size of the implant components greatly affects the results after total knee replacement, and any errors in misplaced use result in double load in the attachment and traction sites of the ligaments (Victor, 2009). This leads to stimulation of stiffness, instability, and early loosening (Berger, Crossett, Jacobs, & Rubash, 1998) and (Tew & Waugh, 1985).

Extensive cases of fatigue fracture of metallic tibial baseplates have been reported in the literature (Abernethy, Robinson, & Fowler, 1996). Most reports relate to fatigue fracture due to insufficient bone support, especially when combined with a distally well fixed stem, increasing the load on the unsupported side of the tray (Flivik, Ljung, & Rydholm, 1990). This situation can occur in some situations. Tibial bone loss can occur due to severe varus or valgus deformities (Chen & Krackow, 1994). The presence of a layer of fibrous tissue between the bone and cement may also produce inadequate support to the tray (Scott, Ewald, & Walker, 1984). Other clinical factors are axial malalignment, overloading due to patient weight and/or high activity level and poor fixation of the tibial component (Abernethy, Robinson, & Fowler, 1996).

Degenerative arthritis of the knee joint affects the line cartilage of the tibia and the femur, and occasionally causes severe pain and may require surgery to replace the knee with artificial components. Artificial joints must meet the design requirements; they should be ergonomic and biocompatible. During activation stresses are developed at the interface of joint. It is important to optimize prosthetic knee joint design to ensure the stress intensity. To this end, finite element analysis is the most powerful numerical tool that can be used to optimize the design (Mallesh & Sanjay , 2012). It is assumed that the materials used in biomaterials are a necessary part of the long survival of the knee implants. Biomaterials must meet the mechanical, biological and physical prerequisites of their expected utilization. In day-to-day activities, knee implant may experience mechanical forces that cause a feeling of pressure, push, pull, twist, or rubbing of components on one another.

In 2003, Mr. Villa et al. (Villa, Migliavacca, Gastaldi, Colombo, & Pietrabissa, 2003) started to estimate the lifetime of the tibial baseplate which was made of CoCrMo empirically and numerically. The mechanical test was carried out in accordance with the ISO 14879-1 standard and was inspired by the loading conditions of Mr. Ahir et al. In 1999 (Ahir, Blunn, Haider, & Walker, 1999) and in parallel, life expectancy was estimated using the finite element analysis and Sines fatigue criteria (Sines & Waisman, 1959). The results of the combine outputs of finite element analysis and Sines fatigue test indicated a significant agreement with the mechanical test results. Also, the location of maximum principal stresses in the tibial baseplate component based on the finite element analysis was the same as the location of failure of this component during the mechanical test.

In 2016, Raul et al. (Rawal, Yadav, & Pare, 2016) by combining the effects of fatigue and wear estimated the life of the knee joint prosthesis. Initially, the finite element analysis was carried out based on the loading conditions of the key points of ISO (Lundberg, Ngai, & Wimmer, 2012) and the contact stresses were extracted and the wear depth was determined with the help of modified form of the classic Archard's Wear Law (Hamilton, Sucec, Fregly, Banks, & Sawyer, 2005). In the following, by using the finite element analysis, the maximum and minimum Von Mises stresses were extracted in the UHMWPE section and the stress amplitude, mean stress and maximum mean stress was calculated in UHWMPE. Ultimately, the lifetime of prosthesis was estimated to be between 13 and 14 years.

The above said points clearly highlight the importance of discussing stress analysis and control of fatigue life and failure in knee implants. Since today knee replacement is also common

in people under 50 years of age, and given the fact that people with lower ages have more severe physical activities than the elderly people, there would be definitely more severe cyclic loading on implants during walking, running, jumping and the like. The study of stress distribution and survival in implants helps to optimize and improve their design. Also, in comparison with laboratory tests these analyzes are very popular and practical due to the cost-effectiveness and the possibility of considering more and varied parameters in finite element analysis.

Therefore, in this study, the distribution of stress and fatigue in the entire implant assembly and life estimation have been investigated by applying the loading of the walking cycle)Lundberg, Ngai & ,Wimmer, 2012(in knee implants using finite element method and cubic mesh technique.

2. Methodology

First, a three-dimensional tibia-and-femur model obtained from the CT scan was entered to Solidworks software. According to the dimensions and properties of the original model, a simplified model was designed. Subsequently, different parts of the implant like tibial and femur components were designed, including the tibia tray and poly insert, as well as collateral ligaments. Then, the entire set assembled in Solidworks was transferred to the analytical software of the finite element of Abaqus to apply the load and analyze the stress. After applying the boundary conditions, the load was applied to the set and the distribution of stress in the implant and bone was determined. Then, using stress distribution results, fatigue life was estimated.

2.1 Finite element analysis

2.1.1 Geometric modeling

First, the three-dimensional model obtained from the knee joint was entered to Abaqus software for analysis by removing meniscus, condyle, patella, platelet tibial, cruciate ligaments and collateral ligaments. The femur and tibia are approximately 83.78 mm and 77.59 mm in length, and 65.06 and 64.81 in width, respectively.

And a three-dimensional model of an implant was designed in Solidworks Software consisting of a femoral component with length and a thickness of 70, and 2 respectively, and a tibial component, including the poly insert, with length, width, and approximate thickness of 85, 60, 5.25 mm and a tibial tray with length, width, and thickness of approximately 85, 60, 5.25 mm respectively. Also a 3D model of the collateral ligament with length and long and short diameter

(an ellipse) of approximately 66, 3.4 and 2.3 mm respectively (Meister, Michael, Moyer, Kelly, & Schneck, 2000) was designed in Solidworks software as well.

Ti6Al4V was chosen for materials manufacturing femur component and the baseplate tray, and for the poly insert of tibia component high molecular weight (between 3 and 6 million) polyethylene was used. In the end, femur component was placed in the lower part of the thigh, tibia tray from the leg part was placed in the tibia bone and the poly insert was placed between the femur component and the tibia tray and doing all this the final assemblage was performed.

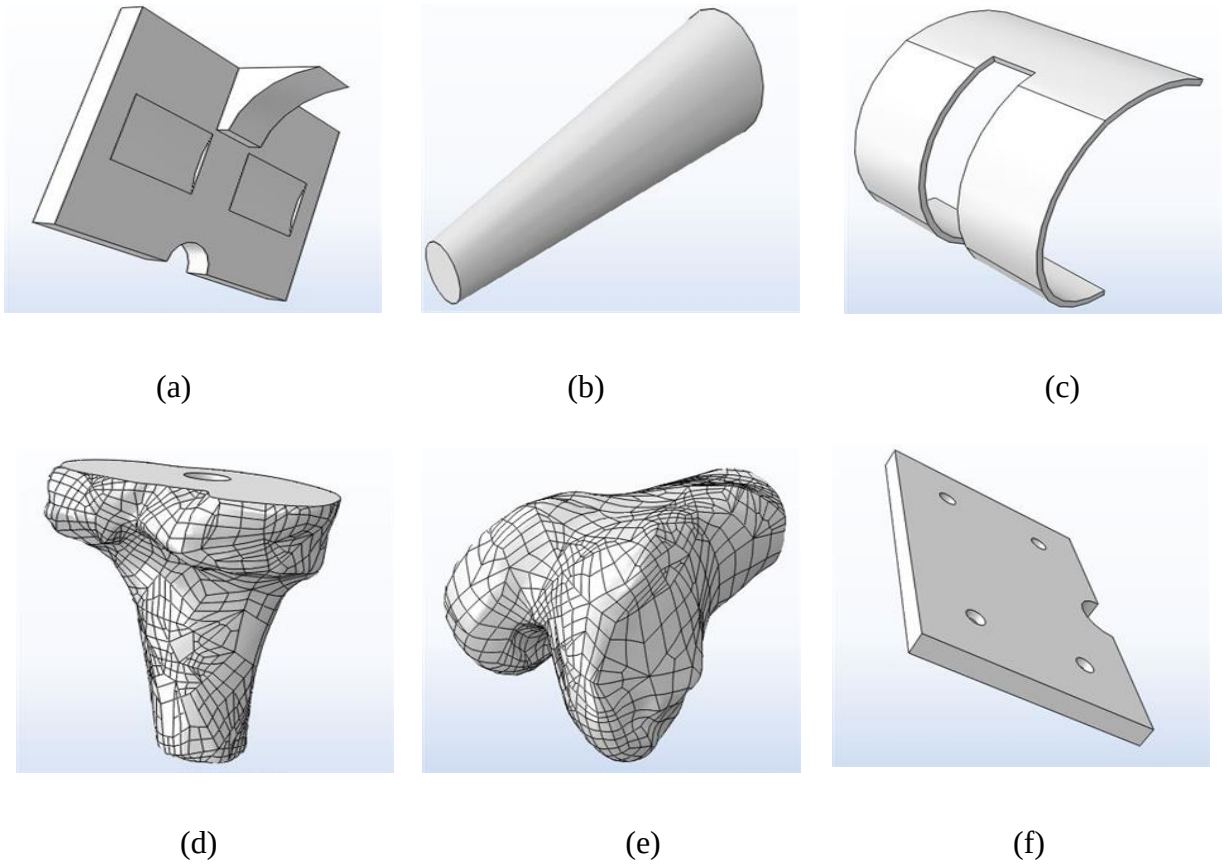

Figure 1: *Seprated 3D Model - **a)**UHMWPE Insert & **b)**Stem & **c)**Femor Component & **d)**Tibia Bone & **e)**Femor Bone & **f)**Tibia Component*

2.1.2 Simulation of finite element

In finite element analysis, the built geometric models were converted into simpler and smaller elements. The finite element model consists of 60446 three-dimensional elements and 137024 nodes including: 1869 C3D20R brick elements and 13816 nodes for femur component implant, 4932 C3D20R cubic element and 25349 nodes for the poly insert of femur component implant, 3732 C3D20R brick elements, and 19612 For baseplate tray implant, 23683 C3D10

tetrahedron element and 35928 for femur bone and 25515 C3D10 tetrahedron element and 38754 for tibia bone. It should be noted that, in the bony areas due to the geometric complexity of the femur and tibia bones, as well as the focus on stress analysis in the implant section, tetrahedron elements were used. The three-dimensional brick elements used in all components were of the standard and quadratic C3D20R elements type, and the final meshing is shown in Fig 3.

Figure 2: *Assembley of complex componenet*

In this study, the femur component and the tibia tray component of the implant made of Ti6Al4V and the poly insert of the tibia component made of ultra-high molecular weight polyethylene were selected for the finite element analysis. The behavior of all materials, including the metal, polyethylene and bone parts, was considered as linear isotropic, and the mechanical properties of these materials are shown in table 1.

In the present study due to the fixability of the hard tissue, the femur component of the implant is completely attached to the thigh bone and baseplate tray component of implant is attached completely to the tibia bone and the bone formation is done completely, therefore, the attachment type of the implant components to the bone was considered to be tie. Due to the integrity of the tibia component of the implant, the poly insert was tied to baseplate tray. Also, between the femur component of the implant and the poly insert, a surface-to-surface contact with friction coefficient of 0.13 was considered (Samadhiya, Yadav, & Rawal, 2014).

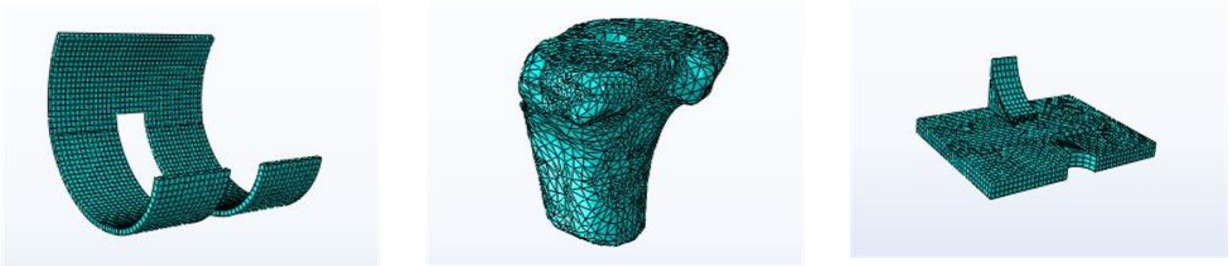

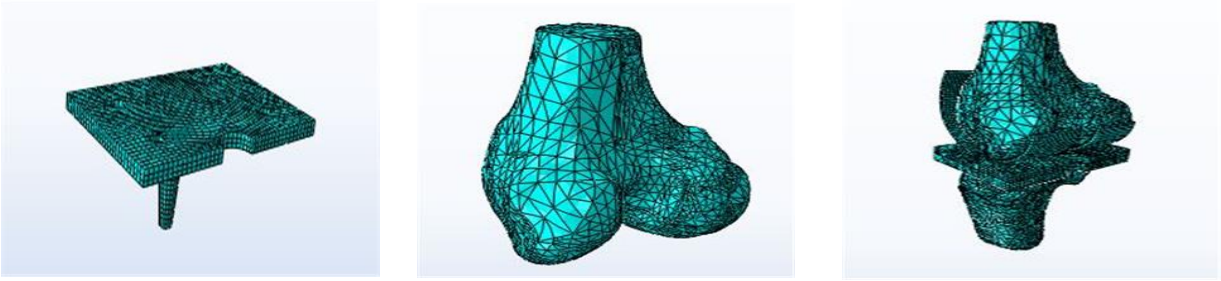

Figure 3: *Finite element model of complex*

2.1.3. Boundary condition and loading

Static and dynamic analyzes of implants should be done around the matter of assurance of designs. Implants usually operate on the basis of static analyzes; static finite element analysis is often performed under the forces of walking, running, jumping, etc. Loading conditions using contact analysis is achieved in finite element models, for this purpose, the target and contact surfaces between the unique parts of the model are specified without the integration of the nodes between the components.

Implant loading was done by applying forces of 200 N and 2,600 N vertically to the metatarsus (Lundberg, Ngai, & Wimmer, 2012). The size of the force, as well as the point of its application, was selected according to the study of Kumbhalkar et al. in 2013 (Kumbhalkar, Nawghare, Ghode, Deshmukh, & Armarkar, 2013)

To apply the boundary conditions, the upper surface of the femur was completely fixed and the force applied to the metatarsus was done as a coupling to the lower surface of the tibia.

3. Checking of convergence of meshing

To ensure the achieved results, checking the convergence of meshing is a necessary step. In the present study, for the purpose of checking the convergence, five different sizes of elements were considered: sizes of 3, 2.5, 2, 1.5, 1.1 mm, respectively.

Then the Von Mises stress results at each step were extracted on a specific path at the most critical node of implant using Abaqus finite element software and then the Von Mises stress diagram was plotted based on the path. By examining the obtained diagram of the results, as seen in Fig 4 the diagram overlaps in sizes of 2 and 2.5 mm, and diverges in the size of 1.1 mm, which means convergence of the 2 mm size, hence the element size of 2 mm was selected for the next investigations.

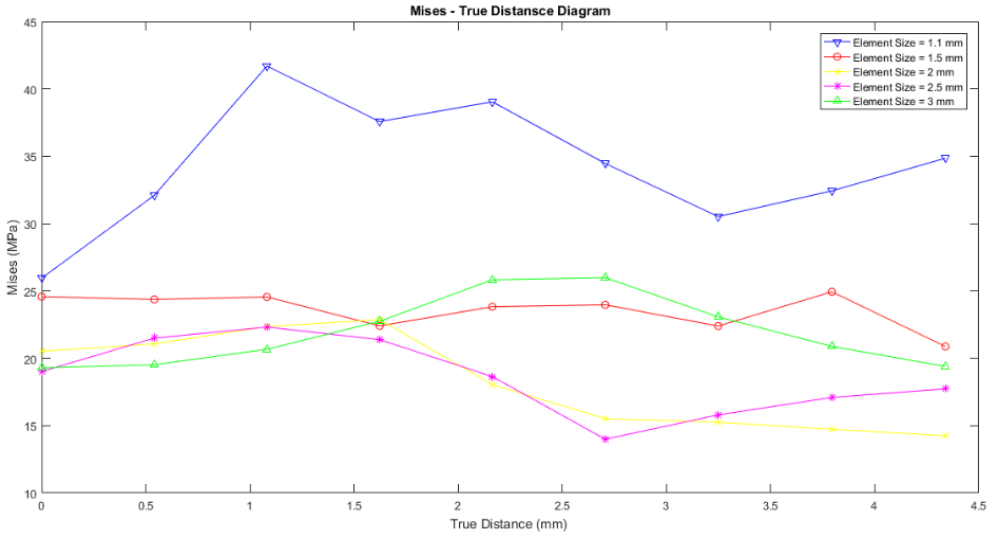

Figure 4: *Mesh Covergence Curve*

4. Findings

4.1 Evaluation of stress distribution in different loadings

After completing the above steps and examining the mesh converge, in two stages of analysis, using different loadings, the stress distribution was investigated and the fatigue life was estimated. As it was predicted, in all analyzes, the maximum stress, occurred in the femur component of the implant. As shown in Table 2 in each of the analyzes, the maximum amount of the Von Mises stress and the maximum principal stress did not reach the yield strength amount of Ti6Al4V (yield strength of Ti6Al4V is 925 MPa).

Table 1: *Mechanical & fatigue properties of Titanium alloy Ti6Al4V (Sterling, Shamsaei, Torries, & Thompson, 2015) & (Navarro , Muñoz , & Domínguez, 2008)*

Material	ν (Poisson ratio)	σ_y (Yield Stress) (MPa)	σ_{ult} (Ultimate Strength) (MPa)	E (Elasticity Module) (GPa)	σ_f' (Fatigue Strength Coefficient)	b (Fatigue Strength Exponent)	ε_f' (Fatigue Ductility Coefficient)	c (Fatigue Ductility Exponent)
Ti6Al4V	0.321	925	965	115.7	1933	-0.1	7.55	-1.29

Regarding the distribution of the stresses shown in Fig 9 the femur component of the implant has the maximum principal stress and the highest fatigue loading can be observed in this

part and therefore it can be selected as a critical point. The critical point is considered to examine fatigue and estimate the life of the implant set.

4.2 Evaluation of the results analysis

To evaluate the results and analyzes, we used the studies of Khaled et al. in 2003 (Khaled , et al., 2014) Kumbhalkar et al. in 2013)Kumbhalkar, Nawghare, Ghode, Deshmukh & , Armarkar, 2013(and Villa et al. in 2014)Villa, Migliavacca, Gastaldi, Colombo & ,Pietrabissa, 2003(. Experimental and laboratory study of Villa was carried out to perform the endurance limit test in accordance with ISO 14879-1, so that for all samples, a compressive wavesine of up to a 7Hz maximum frequency was applied. In accordance with the study after Ahir et al. 1999)Ahir, Blunn, Haider & ,Walker, 1999(the minimum load of 0N and the maximum load of 500, 2000 and 4000N were applied on all samples in order to prevent plastic deformation of the tibial baseplate tray during the test. Likewise fatigue tests were performed until the tibial base plate indicated failure or until five million cycles were achieved. After simulating the loading conditions, regarding the fact that the location of the maximum principal stress obtained from the finite element analysis was in accordance with the failure point of implant in Khaled's study (Khaled , et al., 2014) therefore the results can be considered acceptable.

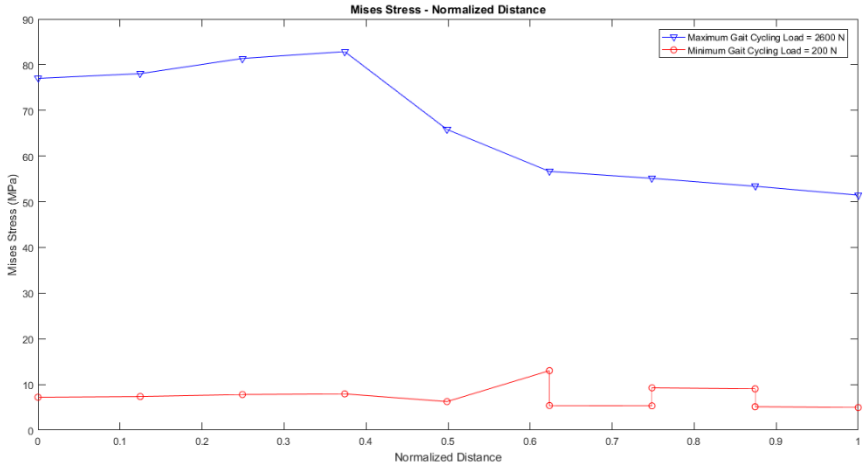

Figure 5*: Von Mises Stress variations curve*

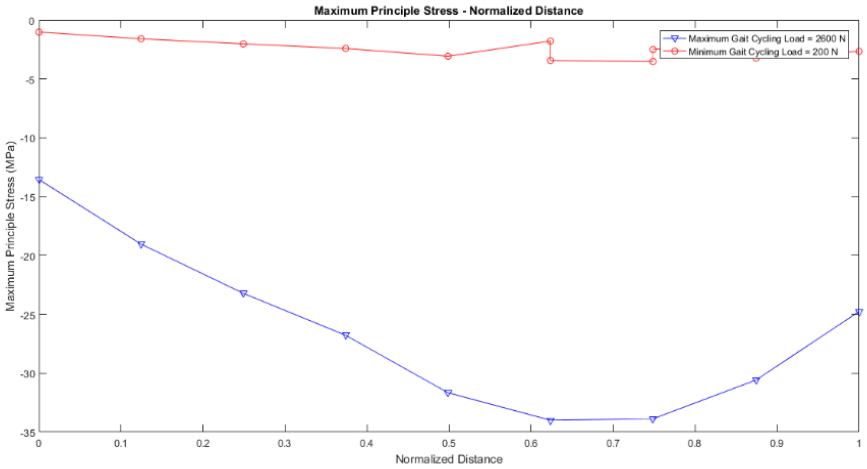

Figure 6: *Max Principal Stress variations curve*

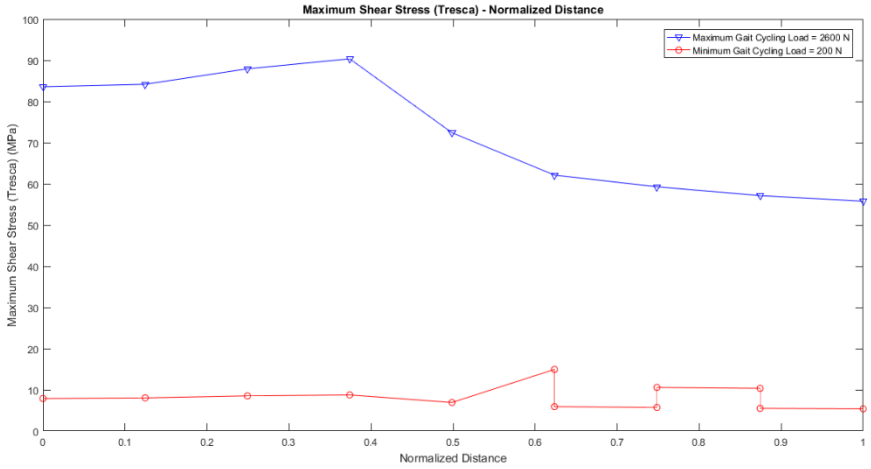

Figure 7: *Max Shear Stress variations curve*

Figure 8: *Fractured specimen in exprimental condition* (Khaled , et al., 2014)

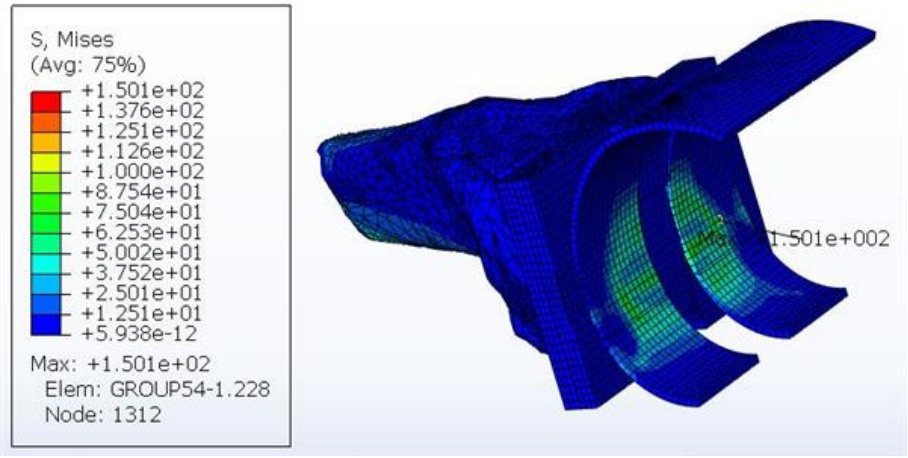

Figure 9: *Analyzed specimen in software comparison with experimental condition*

Table 2: *Maximum values of Max. Principal & Von Mises stress of implant in different Load*

Load (N)	Maximum Principal Stress (MPa)	Maximum Von Misses Stress (MPa)	Maximum Principal Stress to Yield Stress (%) Ratio	Maximum Von Misses Stress to Yield Stress (%) Ratio
200	12.496	13.4231	1.35	1.45
2600	132.537	150.071	14.32	16.22

4.3 Fatigue estimation and life expectancy estimation

A good implant plan should be able to meet unlimited or maximum fatigue life, this can be analyzed and evaluated with laboratory tests or fatigue analyzes. The aim of this study was to analyze and estimate the fatigue life of knee implants using multiaxial fatigue criteria and to compare the results with each other. To this end, we need information about the titanium fatigue properties table 2 as well as the applied stresses on the implant.

Examining the critical stresses indicated that in none of the analyzes, the amount of critical stress in the implant could reach the yield stress of titanium. Thus, in the absence of defects, the Basquin, Coffin Manson, Brown Miller, Fatemi Socie and Smith Watson Topper

Since in this study the mean stress is not equal to zero, we need a modification for the Basquin equation (Dowling , 2003) to enable it to be used in modifying the amount of stress, and to do this we use the Soderberg modification. As noted earlier, the aimed critical location for the analysis of fatigue was located in femur component of the implant.

Maximum stress tensor for maximum loading and minimum stress tensor for minimum loading at the critical point are shown in the (1) and (2).

$$\sigma_{min} = \begin{bmatrix} 33.3403E-03 & 20.8000E-03 & -11.4472E-03 \\ 20.8000E-03 & 91.7590E-03 & 57.9173E-03 \\ -11.4472E-03 & \cdots 57.9173E-03 & -4.62238E-03 \end{bmatrix} \quad (1)$$

$$\sigma_{max} = \begin{bmatrix} 232.497E-03 & 579.594E-03 & -16.5682E-03 \\ 579.594E-03 & 1.72316 & 118.845E-03 \\ -16.5682E-03 & 118.845E-03 & -7.01151E-03 \end{bmatrix} \quad (2)$$

After extracting the maximum and minimum stress tensor from Abaqus software, in order to use the Basquin equation for life estimation, amplitude stress tensor should be converted to a scalar through the Von Mises, the maximum principal stress, and the Tresca criteria.

$$\sigma_a = \sigma_f^{'}(2N_f)^b \quad (3)$$

In equation (3) $\sigma_f^{'}$, b are the constants of Basquin equation that are the fatigue strength coefficient and fatigue strength exponent and were obtained from laboratory tests. The value of these constants for titanium is displayed in table 1.

Due to the need to convert the mean stress tensor into a scalar, this value is obtained by using the mean stress tensor trace divided by 3. Matrix trace is the sum of components in main diagonal.

As mentioned earlier, due to the fact that in the present study the mean stress scalar was not equal to zero, with the help of the Soderberg modification (4), the scalar value of the stress amplitude was corrected and finally, the implant's lifetime was estimated and the result was displayed in table 3.

$$(\sigma_a)_{rev} = \frac{\sigma_a}{1-(\sigma_m/\sigma_f^{'})} \quad (4)$$

For estimating the lifetime by the Coffin Manson criterion (Dowling , 2003), the maximum strain tensor for the maximum loading and the minimum strain tensor for the minimum loading at the critical point can be found in (5) and (6).

$$\varepsilon_{min} = \begin{bmatrix} 30.7785E-09 & 485.454E-09 & -267.167E-09 \\ 485.454E-09 & 712.500E-09 & 1.35174E-06 \\ -267.167E-09 & 1.35174E-06 & -412.229E-09 \end{bmatrix} \quad (5)$$

$$\varepsilon_{max} = \begin{bmatrix} -3.08196E-06 & 13.5272E-06 & -386.688E-09 \\ 13.5272E-06 & 14.3134E-06 & 2.77375E-06 \\ -386.688E-09 & 2.77375E-06 & -5.87692E-06 \end{bmatrix} \quad (6)$$

After extracting the maximum and minimum strain tensor from the Abaqus software, in order to use the Coffin Manson criterion for life estimation, we need to convert the strain amplitude tensor to a scalar through maximum principal strain.

$$\varepsilon_a = \frac{\sigma_f'}{\mathrm{E}}(2N_f)^b + \varepsilon_f'(2N_f)^c \qquad (7)$$

In equation (7) σ_f', b, ε_f' and c are the Coffin Manson constants that are fatigue strength coefficient, fatigue strength exponent, fatigue ductility coefficient and, fatigue ductility exponent respectively which are obtained from laboratory tests. The values of these constants for titanium are displayed in table 1.

Due to the need to convert the mean strain tensor into a scalar, this value is obtained by using the mean strain tensor trace divided by 3. Matrix trace is the sum of components in main diagonal.

Finally, the lifetime of implant was estimated using the Coffin Manson's criterion and the result is displayed in table 3.

For life estimation based on Brown Miller's critical plane criterion (Brown & Miller, 1973), first it is necessary to determine the normal value of the plane in which the shear strain is maximum. For this purpose, Eigen values and directions corresponding to those values in strain amplitude were determined and, with the help of the 45 degree rotation tensor, around the perpendicular axis to the plane, including the corresponding vectors to the maximum and minimum values of the Eigen values of the strain tensor, the normal value of the plane was determined.

The value of $\Delta\varepsilon_n$ is obtained from multiplying normal transpose in the difference between the maximum and minimum strain tensor in normal. The value of γ_{max} is equal to the difference between the maximum and minimum of the Eigen value of stress amplitude tensor divided by 2.

$$\gamma_{max} + \frac{\Delta\varepsilon_n}{2} = 1.65\frac{\sigma_f'}{\mathrm{E}}\left(2N_f\right)^b + 1.75\varepsilon_f'\left(2N_f\right)^c \qquad (8)$$

In equation (8) σ_f', b, ε_f' and c are the Brown Miller constants that are fatigue strength coefficient, fatigue strength exponent, fatigue ductility coefficient and, fatigue ductility exponent respectively which are obtained from laboratory tests. The values of these constants for titanium are displayed in table 1.

In the lifetime estimation based on the critical plane of Fatemi Socie's criterion (Fatemi & Socie, 1988), the determination of the normal of the plane in which the shear strain is maximized is exactly similar to that used in Brown Miller's criterion. The value of ${\sigma_n}^{max}$ is obtained from multiplying normal transpose in the maximum stress tensor in normal. The value of γ_{max} is equal to the difference between the maximum and minimum of the Eigen value of stress amplitude tensor divided by 2.

$$\gamma_{max}\left(1+\frac{0.6{\sigma_n}^{max}}{\sigma_y}\right)=1.29\frac{\sigma_f^{'}}{\mathrm{E}}\left(2N_f\right)^b+0.387\frac{{\sigma_f^{'}}^2}{\mathrm{E}\sigma_y}\left(2N_f\right)^{2b}+1.50\varepsilon_f^{'}\left(2N_f\right)^c+0.45\frac{\varepsilon_f^{'}\sigma_f^{'}}{\sigma_y}\left(2N_f\right)^{b+c} \quad (9)$$

In equation (9) $\sigma_f^{'}$, b, $\varepsilon_f^{'}$ and c are the Fatemi Socie's constants that are fatigue strength coefficient, fatigue strength exponent, fatigue ductility coefficient and, fatigue ductility exponent respectively which are obtained from laboratory tests. The values of these constants for titanium are displayed in table 1.

For life estimation based on Smith Watson Topper's critical plane criterion (Smith, Watson, & Topper, 1970) , to determine the normal of the plane in which the maximum principal strain range occurs the Eigen values of the difference between the maximum and minimum strain tensor were determined and finally the normal of the plane will be equal to the Eigen vector correspondent to the maximum Eigen value of the difference of maximum and minimum strain tensor. The value of ${\sigma_n}^{max}$ is obtained from multiplying normal transpose in maximum strain tensor in normal. The value of $\Delta\varepsilon_1$ is equal to the difference between the maximum and minimum of the Eigen value of stress amplitude tensor.

$$\frac{{\sigma_n}^{max}\Delta\varepsilon_1}{2}=\frac{{\sigma_f^{'}}^2}{\mathrm{E}}(2N_f)^{2b}+\varepsilon_f^{'}\sigma_f^{'}(2N_f)^{b+c} \quad (10)$$

In equation (10) $\sigma_f^{'}$, b, $\varepsilon_f^{'}$ and c are the Smith Watson Topper's constants that are fatigue strength coefficient, fatigue strength exponent, fatigue ductility coefficient and, fatigue ductility exponent respectively which are obtained from laboratory tests. The values of these constants for titanium are displayed in table 1.

Table 3: *Fatigue life estimation according to multiaxial criteria*

Multiaxial Fatigue Criteria	Fatigue Life Estimation (Cycle)
Basquin - Von Mises	$8.9922 * 10^{32}$
Basquin - Maximum Principal Stress	$8.9807 * 10^{32}$
Basquin - Maximum Principal Stress (Tresca)	$8.077 * 10^{35}$
Cofin Manson - Maximum Principal Strain	$5.7573 * 10^{31}$
Brown Miller (Critical Plane Fatigue Criteria)	$8.7307 * 10^{31}$

Fatemi Socie (Critical Plane Fatigue Criteria)	$1.3018 * 10^{34}$
Smith Watson Topper (Critical Plane Fatigue Criteria)	$4.1438 * 10^{29}$

5. Discussion and conclusion

The purpose of this study was to estimate the life of knee implants by walking cycle loads. At first, distribution of stress in the implant was investigated in two different conditions, and then the implant's life estimation using critical stress areas and using the titanium fatigue properties was evaluated. The most important results from this study are as follows:

With the maximum and minimum loading of the walking cycle it was observed that the maximum stress occurs for both of the loadings exactly in the same point on the crescent part of the femur component of implant. It can be concluded that with the continuation of fatigue loading, the maximum stresses are concentrated in this area, and these areas have the shortest life span than other areas. Also in reality it is observable that most of the implants are broken down from the crescent part of their femur component.

According to the results of life estimation based on multiaxial fatigue criteria, the maximum life was related to the maximum shear stress (Tresca) and the shortest life was that of the Smith Watson Topper's criterion. The results of the Von Mises criteria and the maximum main stresses are very close and almost in line with each other, and the results of the maximum principal strain and Brown Miller's one are relatively close to each other. Due to the results, implants have unlimited life.

6. Suggestions for further studies

Considering the point that no pieces and equipment are free of defects in the microstructure, it is suggested that the implant's life should be evaluated based on the existence of cracks in the piece. In addition, considering the importance and impact of bone in predicting fatigue life, it is suggested to investigate the gender and bone loss impact on implant life. And finally the effect of using different materials in the structure of knee implants in the estimation of fatigue life can be studied as well.

References

Abernethy, P. J., Robinson, C. M., & Fowler, R. M. (1996). Fracture of the metal tibial tray after Kinematic total knee replacement. Journal of Bone and Joint Surgery, 78B (2), 220-225. https://doi.org/10.1302/0301-620X.78B2.0780220

Ahir, S. P., Blunn, G. W., Haider, H., & Walker, P. S. (1999). Evaluation of a testing method for the fatigue performance of total knee tibial trays . Journal of Biomechanics , 32, 1049-1057. https://doi.org/10.1016/S0021-9290(99)00094-9

Berger, R. A., Crossett, L. S., Jacobs, J. J., & Rubash, H. E. (1998). Malrotation causing patellofemoral complications after total knee arthroplasty. Clinical orthopaedics and related research, 356, 144-153. https://doi.org/10.1097/00003086-199811000-00021

Brown, M. W., & Miller, K. J. (1973). A Theory for Fatigue Failure under Multiaxial Stress-Strain Conditions. Proceedings of the Institution of Mechanical Engineers, 187 (1), 745-755 . https://doi.org/10.1243/PIME_PROC_1973_187_161_02 https://doi.org/10.1243/PIME_PROC_1973_187_161_02

Chen, F., & Krackow, K. A. (1994). Management of tibial defects in total knee arthroplasty. Clinical Orthopaedics and Related Research, 305, 249-257. https://doi.org/10.1097/00003086-199408000-00031

Dowling, N. (2003). Mechanical Behavior of Materials Engineering Methods for Deformation, Fracture, and Fatigue . Angshuman Chakraborty.

Fatemi, A., & Socie, D. (1988). A Critical Plane Approach to Multiaxial Fatigue Damage Including Out-Of-Phase Loading. Fatigue & Fracture of Engineering Materials & Structures, 11(3), 149–165. https://doi.org/10.1111/j.1460-2695.1988.tb01169.x

Flivik, G., Ljung, P., & Rydholm, U. (1990). Fracture of the tibial tray of the PCA knee: a case report of early failure caused by improper design. Acta Orthopaedica Scandanavica , 61(1), 26-28. https://doi.org/10.3109/17453679008993059

Hamilton, M. A., Sucec, M. C., Fregly, B. J., Banks, S. A., & Sawyer, W. G. (2005). Quantifying multidirectional sliding motions in total knee replacements. Journal of Tribology, 127(2), 280-286. https://doi.org/10.1115/1.1843136

Khaled , M., Sarraf, F., Rupert Wharton, M., Hani , B., Abdul-Jabar, M., Guarangkumar Shah, F., . . . Singer, F. (2014). Fatigue Fractures of Total Knee Prostheses A Cause of Knee Pain. Bulletin of the Hospital for Joint Diseases, 72(3), 242-246.

Kumbhalkar, M. A., Nawghare, U., Ghode, R., Deshmukh, Y., & Armarkar, B. (2013). Modeling and Finite Element Analysis of Knee Prosthesis with and without Implant. Universal Journal of Computational Mathematics , 1(2), 56-66. doi:10.13189/ujcmj.2013.010204

Lundberg, H. J., Ngai, V., & Wimmer, M. A. (2012). Comparison of ISO Standard and TKR Patient Axial Force Profiles during the Stance Phase of Gait,. Proc Inst Mech Eng H, 226(3), 227–234. https://doi.org/10.1177/0954411911431650

Mallesh, G., & Sanjay , S. J. (2012). Finite Element Modeling and Analysis of Prosthetic Knee Joint. International Journal of Emerging Technology and Advanced Engineering, 2(8), 264-269.

Meister, B., Michael, S., Moyer, R., Kelly, J., & Schneck, C. (2000). Anatomy and Kinematics of the Lateral Collateral Ligament of the Knee. The American Journal of Sports Medicine, 28(6), 869-878. https://doi.org/10.1177/03635465000280061601

Navarro , C., Muñoz , S., & Domínguez, J. (2008). On the use of multiaxial fatigue criteria for fretting fatigue life assessment. International Journal of Fatigue, 30(1), 32-44. doi: https://doi.org/10.1016/j.ijfatigue.2007.02.018

Ranawat, A. A., & Ranawat, C. S. (2012). The history of total knee arthroplasty. The Knee Joint, 699-707 . https://doi.org/10.1007/978-2-287-99353-4_63

Rawal, B. R., Yadav, A., & Pare, V. (2016). Life estimation of knee joint prosthesis by combined effect of fatigue and wear. Procedia Technology, 23, 60-67. https://doi.org/10.1016/j.protcy.2016.03.072

Samadhiya, S., Yadav, A., & Rawal, B. R. (2014). Biomechanical Analysis of Different Knee Prosthesis Biomaterials Using Fem. Journal of Mechanical and Civil Engineering (IOSR-JMCE), 11(3), 120-128. https://doi.org/10.9790/1684-1134120128

Scott, R. D., Ewald, F. C., & Walker, P. S. (1984). Fracture of the metal tray following total knee replacement. Journal of Bone and Joint Surgery, 66A(5), 780-782. https://doi.org/10.2106/00004623-198466050-00021

Sines, G., & Waisman, G. (1959). Behaviour of Metals Under Complex Stating and Alternating Stresses in Metal Fatigue. New York: McGraw Hill.

Smith, K. N., Watson, P., & Topper, T. H. (1970). A stress-strain function for fatigue of metals. Journal of Materials, 5(4), 767–778.

Sterling, A., Shamsaei, N., Torries, B., & Thompson, S. (2015). Fatigue Behaviour of Additively Manufactured Ti-6Al-4V. Procedia Engineering, 133, 576-589. https://doi.org/10.1016/j.proeng.2015.12.632

Tew, M., & Waugh, W. (1985). Tibiofemoral alignment and the results of knee replacement. Journal of Bone & Joint Surgery, 67(4), 551-556. https://doi.org/10.1302/0301-620X.67B4.4030849

Victor, J. (2009). A comparative study on the biomechanics of the native human knee joint and total knee arthroplasty. Doctoral dissertation, https://lirias.kuleuven.be/handle/123456789/233948S, 135–137.

Villa, T., Migliavacca, F., Gastaldi, D., Colombo, M., & Pietrabissa, R. (2003). Contact stresses and fatigue life in a knee prosthesis: comparison between in vitro measurements and computational simulations. Journal of Biomechanics, 37, 45–53. https://doi.org/10.1016/S0021-9290(03)00255-0